Decoding motor neuron activity from epimysial thin-film electrode recordings following targeted muscle reinnervation

Decoding motor neuron activity from epimysial thin-film electrode recordings following targeted muscle reinnervation

OPEN ACCESS
IOP Publishing

Made open access 10 April 2019
Journal of Neural Engineering

J. Neural Eng. **16** (2019) 016010 (9pp)
https://doi.org/10.1088/1741-2552/aaed85

Decoding motor neuron activity from epimysial thin-film electrode recordings following targeted muscle reinnervation

Silvia Muceli[1], Konstantin D Bergmeister[2], Klaus-Peter Hoffmann[3], Martin Aman[2], Ivan Vukajlija[1], Oskar C Aszmann[2,4] and Dario Farina[1,5]

[1] Department of Bioengineering, Imperial College London, London, United Kingdom
[2] Christian Doppler Laboratory for Restoration of Extremity Function, Medical University of Vienna, Vienna, Austria
[3] Department of Medical Engineering and Neuroprosthetics, Fraunhofer Institute for Biomedical Engineering, St Ingbert, Germany
[4] Department of Surgery, Division of Plastic and Reconstructive Surgery, Medical University of Vienna, Vienna, Austria

E-mail: d.farina@imperial.ac.uk

Received 25 July 2018, revised 10 October 2018
Accepted for publication 1 November 2018
Published 12 December 2018

Abstract

Objective. Surface electromyography (EMG) is currently used as a control signal for active prostheses in amputees who underwent targeted muscle reinnervation (TMR) surgery. Recent research has shown that it is possible to access the spiking activity of spinal motor neurons from multi-channel surface EMG. In this study, we propose the use of multi-channel epimysial EMG electrodes as an interface for decoding motor neurons activity following TMR. *Approach.* We tested multi-channel epimysial electrodes (48 detection sites) built with thin-film technology in an animal model of TMR. Eight animals were tested 12 weeks after reinnervation of the biceps brachii lateral head by the ulnar nerve. We identified the position of the innervation zone and the muscle fiber conduction velocity of motor units decoded from the multi-channel epimysial recordings. Moreover, we characterized the pick-up volume by the distribution of the motor unit action potential amplitude over the epimysium surface. *Main results.* The electrodes provided high quality signals with average signal-to-noise ratio >30 dB across 95 identified motor units. The motor unit action potential amplitude decreased with increasing distance of the electrode from the muscle fibers ($P \ll 0.001$). The decrease was more pronounced for bipolar compared to monopolar derivations. The average muscle fiber conduction velocity was 2.46 ± 0.83 m s^{-1}. Most of the neuromuscular junctions were close to the region where the nerve was neurotized, as observed from the EMG recordings and imaging data. *Significance*. These results show that epimysial electrodes can be used for selective recordings of motor unit activities with a pick-up volume that included the entire muscle in the rat hindlimb. Epimysial electrodes can thus be used for detecting motor unit activity in muscles with specific fascicular territories associated to different functions following TMR surgery.

Keywords: targeted muscle reinnervation, motor neuron, man–machine interface, prostheses, EMG, epimysial electrode

(Some figures may appear in colour only in the online journal)

[5] Department of Bioengineering, Imperial College of Science, Technology and Medicine, London SW7 2AZ, United Kingdom.

1. Introduction

Targeted muscle reinnervation (TMR) consists in surgically connecting the nerves that originally innervated muscles in a missing limb into those of remnant muscles above the amputation (Hoffer and Loeb 1980, Kuiken *et al* 2007, 2009). The reinnervated muscles produce electrical activity triggered by the action potentials of the reinnervating axons and therefore amplify the motor neuron activity. The muscle electrical activity is then probed with electrodes and in principle constitutes a window into the output circuitries of the spinal cord, alternative to directly interfacing severed axons of amputated nerves. The electromyographic (EMG) signals following TMR are used for prosthesis control, usually with direct association of the EMG amplitude in a pair of reinnervated sites to the control of a prosthesis degree of freedom (Kuiken *et al* 2007). With this approach, the interference EMG signals represent the strength of the neural drives from the pools of reinnervating motor neurons.

Once a neuromuscular junction is established, there is a one-to-one association between an axonal action potential and the compound action potential in the innervated muscle fibers. Therefore, the interference EMG signal is the convolutive mixture of the spike trains of the innervating axons (Farina and Holobar 2016). Recently, it has been shown that this mixture of signals can be decoded with the accurate identification of the neural sources, i.e. the motor neuron spike trains (Farina and Holobar 2016). With this approach, it is possible to directly access the spiking activity of motor neurons and thereby to establish a neural interface via the remaining stump muscles (Farina *et al* 2017b).

We have recently demonstrated the concept of a man-machine interface based on TMR, multi-channel EMG decomposition, and mapping of motor neuron spike trains into prosthesis control (Farina *et al* 2017b, Kapelner *et al* 2018). Moreover, we have shown that motor neurons following TMR are controlled by the central nervous system according to the same physiological principles of rate coding and recruitment as in natural innervation (Farina *et al* 2017a). The perspective of this approach is to establish a high-information transfer interface as a combination of surgery, biological amplification of neural activity, muscle probing, and neural decoding (Bergmeister *et al* 2017, Vujaklija *et al* 2017). While we have shown the clinical feasibility of this approach in humans using non-invasive muscle interfacing (Farina *et al* 2017b), the long-term vision is to chronically implant multi-channel EMG sensors into muscles to establish an interface that is robust over time, overcoming the several drawbacks of non-invasive sensing (Bergmeister *et al* 2017).

As a potential means for chronic muscle recordings, we have developed implantable multi-channel muscle sensors based on thin-film technology that can be inserted intramuscularly. We have tested these systems in animals and healthy humans with acute implants (Farina *et al* 2008, Muceli *et al* 2015). In this paper, we present the use of thin-film electrodes for epimysial multi-channel EMG recordings following TMR and we prove that this interfacing approach allows for the identification of spike trains of motor neurons. As a first step towards clinical implementation of this concept, we present data on an animal preparation. For the first time, we show multi-channel (>40 channels) epimysial EMG signals from surgically reinnervated muscles and their accurate and robust decoding into the discharges of the reinnervating motor neurons. The aims of the study were (i) to prove that the selectivity of epimysial recordings is suitable for detecting individual motor unit activity, and (ii) to investigate the recording volume of this type of electrodes. For these purposes, we identified the position of the innervation zone and the muscle fiber conduction velocity of motor units extracted from the multi-channel epimysial recordings. Moreover, the pick-up volume was characterized by the distribution of the motor unit action potential amplitude over the epimysium surface. The results are a step forward towards the human implantation of muscle sensors for the establishment of a clinical interface with the spinal cord for prosthesis control.

2. Materials and methods

2.1. TMR surgery

Eight Sprague-Dawley (first group) and four Thy1-GFP rats (second group) (male, aged 8–10 weeks) underwent TMR surgery. The first group of animals was used for EMG recordings and the second group for imaging the neuromuscular junctions (Moore *et al* 2012).

Interventions were conducted under general anaesthesia/analgesia using Ketamine/Xylazine i.p. inhalative isoflurane, and Piritramide injections. On the first postoperative days, the drinking water was mixed with Piritramide and glucose for pain relief. Euthanasia was performed under general anaesthesia with a 1 ml intracardial injection of Pentobarbital. All animals received care in compliance with the principles of laboratory animal care as recommended by FELASA. Approval was obtained from the ethics committee of the Medical University of Vienna and the Austrian Ministry for Research and Science (BMWF: reference number: BMWF-66.009/0222-WF/II/3b/2014).

The ulnar nerve was transferred to the lateral head of the biceps brachii muscle following the surgical procedure described in Bergmeister *et al* (2016). In brief, an incision was made on the upper limb from the pectoral muscle to the medial epicondyle of the humerus. First, the motor branch of the musculocutaneous nerve innervating the biceps lateral head was resected. The ulnar nerve was exposed, cut proximal to the medial epicondyle, and neurotized to the epimysium of the motor branch's insertion point via two 11-0 (Ethilon, Ethicon, Johnson and Johnson Medical Care) sutures.

In the second group of animals, muscles were harvested 12 weeks after surgery to allow for sufficient reinnervation and cut in 300 μm slides. Slides were washed for 10 min using PBST, blocked for two hours with blocking buffer (PBST with 10% goat serum and 1% bovine serum albumin), and immersed in a conjugate of α-Bungarotoxin and Alexa Fluor 594 (Life technologies, cat # B-13423) diluted (1:100) in blocking buffer for 16 h. Slides were then covered with fluorescent mounting medium (DAKO, Austria) and coverslips,

and imaged using a Leica confocal and multiphoton microscope with two spectral windows for GFP and Alexa-Fluor 594. In the slides, stained neuromuscular junctions appeared red fluorescent and the axons green fluorescent.

2.2. Epimysial recordings

The EMG recordings were performed twelve weeks after surgery using the electrodes described in Muceli *et al* (2015). These electrodes are constructed on a thin-film substrate of polyimide with an embedded linear array of 16 platinum detection sites with 1 mm inter-site distance. The substrate is 20 μm thick and the detection sites are oval with axes 140 μm and 40 μm. The electrodes have been previously applied for intramuscular recordings (Muceli *et al* 2015, Luu *et al* 2018), and are also suitable for epimysial recordings, which were tested for the first time in this study. Their substrate material and thickness provide optimal flexibility to comply with the muscle shape, making them suitable for both epimysial and intramuscular recordings.

An incision was made on the upper limb from the pectoral muscle to the medial epicondyle of the humerus to expose the biceps lateral head. An 18-gauge cannula was placed at the left anterior paw to anchor the preparation and prevent movement of the experimental setup during muscle contraction. Three epimysial electrodes were mounted on the muscle, two in the most lateral and medial portions of the biceps lateral head and the third one in-between, aligned with the muscle fiber direction (figure 1). Electrode arrays were aligned with the muscle fibers under maximum optical magnification of a surgical operation microscope (Zeiss S88, Munich, Germany). With the described arrangement, the distance between the epimysial electrodes was about 40% of the muscle circumference (c) which was about 2 cm. The linear array of detection sites extended over 1.5 cm covering the entire length of the muscle (figure 1). With this arrangement, we hypothesized that the detection volume of the electrodes corresponded approximately to the full muscle (this was tested in the Results).

Asynchronous motor unit activity was elicited by crushing the ulnar nerve with a microsurgical needle holder (Farina *et al* 2008). This modality allows for the generation of motor neuron action potentials that can be individually identified, contrary to the compound potential of fully synchronous motor neuron activity elicited by electrical stimulation of the nerve. The nerve was progressively crushed from proximal to distal locations. The resulting 48 EMG signals were amplified and recorded with a multi-channel amplifier (OT Bioelettronica, Torino, Italy) in monopolar derivation with respect to a common distant electrode. The sampling frequency was set to 10 240 Hz and data were A/D converted on 12 bits.

2.3. Data analysis

The raw monopolar EMG signals (figure 2) were decomposed into the constituent motor unit action potentials using the EMGLAB software (McGill *et al* 2005). Although this decomposition algorithm allows multi-channel decomposition, each channel was decomposed independently from the others. The firing patterns identified in each channel were used to trigger an average multi-channel template. An action potential was deemed to belong to the same motor unit if the shape and amplitude were consistent across all channels of the three epimysial electrodes. Since the muscle contractions elicited via mechanical stimulation of the nerve (as in the current experiment) are highly variable in duration and usually relatively brief, in some cases only a few discharges could be used for the averaging of the action potentials (see results). For this reason, only discharges that did not overlap in time with those of other motor units were selected for the spike triggered averaging of individual motor unit action potentials. Single differential signals were obtained via software to investigate action potential propagation along the muscle fibers.

When an axonal action potential reaches the muscle at the neuromuscular junction, the muscle action potential propagates in the two directions towards the tendons. Therefore, when the single differential signal is recorded with a linear array of electrodes positioned along the muscle fibers, the action potential propagation may be observed as a translation in time of the motor unit action potential (Masuda *et al* 1983, Merletti *et al* 2003). This results in a typical spatio-temporal profile as represented in figure 3(A). The signals recorded in proximity of the innervation zone have opposite phases due to the generation of the two propagating waves in opposite directions. The signals detected between the innervation zone and tendon regions have similar shape but are delayed in time due to the propagation at constant velocity. At the tendons, the action potentials extinguish, which is often associated to the presence of signal components that are similar across channels with no delay (non-propagating components (Dimitrov and Dimitrova 1974, Farina *et al* 2004)).

The location of the neuromuscular junctions of the muscle fibers in individual motor units (innervation zones) and the action potential conduction velocity were estimated from the signals of the epimysial electrode system corresponding to the maximal amplitude of the motor unit action potential (reference epimysial electrode). The location of the innervation zone was identified as between the two channels of the array where the action potential changed polarity.

To confirm the distribution of the neuromuscular junctions within the muscle, the four Thy1-GFP transgenic rats expressing GFP in neurons and axons were used to image the axons of motor neurons innervating the target muscle at the nerve's insertion into the target muscle. Images were visually inspected to identify the distribution of the neuromuscular junctions along the longitudinal direction of the muscle.

For estimating the propagation velocity of muscle fiber action potentials, two to three channels (proximal or distal to the innervation zone) with clear propagating components were identified from the reference epimysial electrode. The algorithm described in Farina *et al* (2001) was used for the estimation of the propagation delay. The inter-site distance (1 mm) was then divided by the propagation delay to obtain the action potential conduction velocity.

The most proximal of the channels used for estimating conduction velocity was used to calculate the peak-to-peak

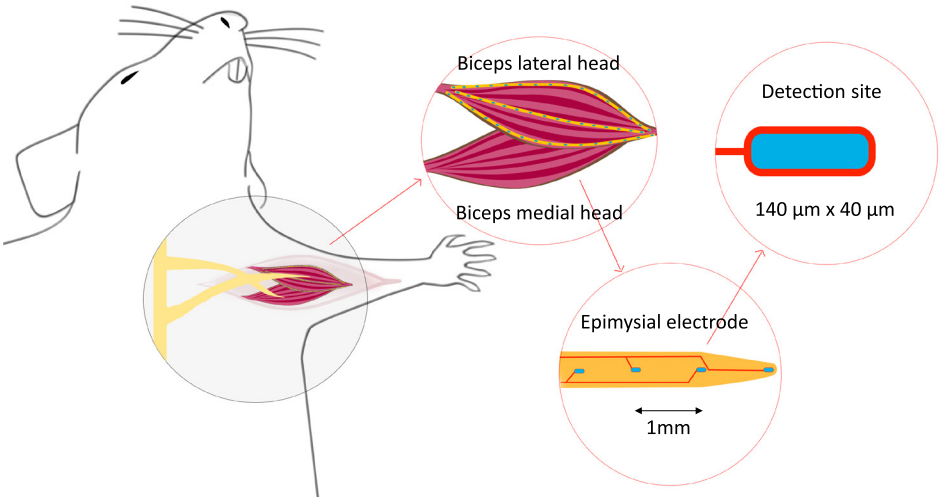

Figure 1. Experimental setup. Following TMR surgery, the rat lateral head of the biceps muscle was reinnervated by the ulnar transfer. The reinnervated muscle was exposed and three epimysial electrodes were positioned on the muscle epimysium in the most lateral and medial position and in-between the two from tendon to tendon in order to cover the whole portion of the exposed muscle. Each epimysial electrode had 16 oval platinum detection sites (with axes 140 and 40 μm) arranged in a linear configuration, at 1 mm distance from each other.

amplitude in the reference epimysial electrode. The corresponding channel at the same distance from the innervation zone was identified in the other two epimysial electrodes to study the decay of signal amplitude with distance. For this purpose, the amplitude at the distant electrodes was expressed as a percentage of the amplitude in the reference epimysial electrode. The normalized amplitude decay was computed for both single differential and monopolar derivations. Amplitude data were tested for normality using the Lilliefors' test. Since the data were not normally distributed (see section 3.2), non-parametric statistics was applied. We compared the single differential and monopolar amplitudes at the same distance from the reference electrode (0.2c and 0.4c) applying the Kruskal–Wallis test. The same test was also used to test if amplitude changed with the distance from the reference electrode. Separate tests were performed for the single differential and monopolar derivations. Statistical significance was set to $P < 0.05$.

2.4. Noise level

Quality of the epimysial recording was quantified by means of the noise level (root mean square) across five central channels of each electrode. The remaining channels close to the proximal and distal tendons were excluded from this analysis because in a few cases they corresponded to detection sites outside the muscle. The root mean square of the noise signal was computed from 1-s intervals and averaged across the five selected channels before and after nerve crushing so that EMG activity was absent.

3. Results

3.1. Innervation zone and conduction velocity

Figure 2 shows an example of signals recorded with the three electrodes during a nerve crush. A total of 95 motor units were identified from the eight animals of the first group (range, 5–24, mean ± standard deviation, 11.9 ± 5.7 motor units per animal). Figure 3(A) shows the single differential montage applied to the linear array of detection sites extending from tendon to tendon of the biceps lateral head. The grey traces represent the shimmer plot of the occurrences of the firings of the same motor unit that were used in the spike-triggered averaging procedure for obtaining the action potential template (black). The number of discharges of individual motor units that were used for the spike triggered averaging varied widely between 2 and 101 (6 ± 12 on average).

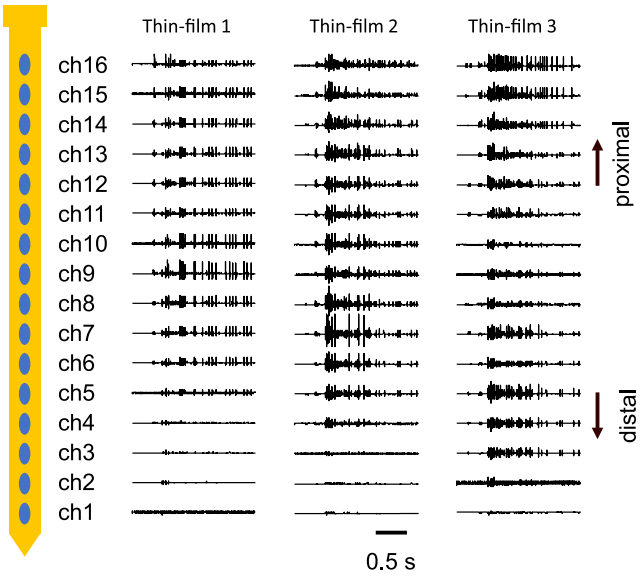

Figure 2. Example of 48 monopolar signals (16 channels per electrode) recorded during a nerve crush.

In the example of figure 3(A), the central epimysial electrode array was chosen as reference electrode, because the motor unit action potential had the highest amplitude. The corresponding innervation zone was identified between

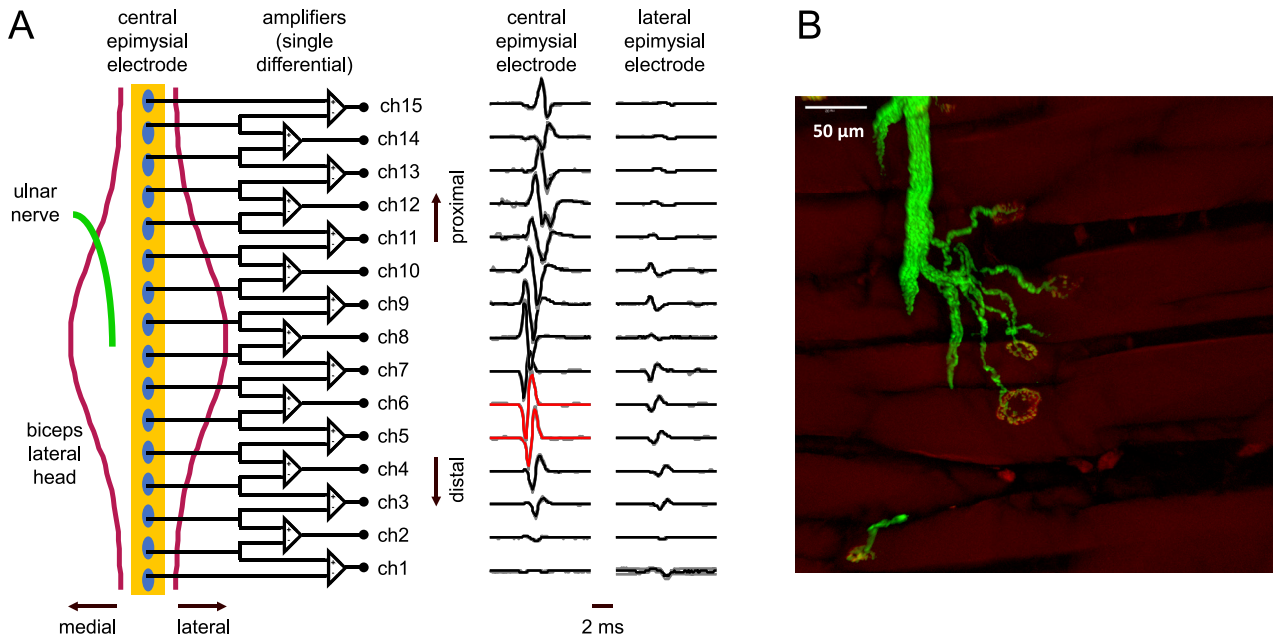

Figure 3. (A) Representative example of a multi-channel single differential template of a motor unit action potential recorded from two epimysial electrodes (16 detection sites each) in the central and lateral portion of the lateral head of the biceps muscle. Only the central electrode is represented on the muscle for clarity. Single differential signals were obtained from the 16 detection sites for the calculation of muscle fiber conduction velocity. Grey traces represent the shimmer plot obtained overlapping the signal segments corresponding to all occurrences of motor unit discharges identified for this representative motor unit. The black traces are templates obtained by averaging the traces of the shimmer plot. The motor unit action potential changed phase between channels seven and eight where the innervation zone was located for that motor unit. Red traces correspond to the signals selected for the calculation of the conduction velocity. (B) Representative images obtained from a stained muscle slice. The nerve axons appear green fluorescent whereas the neuromuscular junctions are red.

the single differential channels seven and eight. Figure 3(B) shows an image from a Thy1-GFP rat, where in green we can observe the axon entering the muscle and in red the neuromuscular junction. Imaging data from the four Thy1-GFP rats showed that most of the neuromuscular junctions were close to the region where the nerve was neurotized (figure 3(B)). This finding was confirmed from the distribution of the innervation zone as obtained from EMG data in the first group of eight animals. Figure 4 shows the histogram of the position of the innervation zone of all identified motor units from the eight animals. In the x-axis, zero represents the median innervation zone for each reference electrode (the electrode where a motor unit was represented with the highest amplitude of its action potential) and corresponded to the position where the nerve entered the muscle, as assessed by visual inspection. The histogram shows that the spread of the innervation zone was usually within three channels, corresponding to twice the inter-site distance, i.e. 2 mm. Only two motor units were innervated at further distance. The average muscle fiber conduction velocity across the 95 motor units was 2.46 ± 0.83 m s^{-1}.

3.2. Action potential amplitude

Figure 5 shows the distribution of the action potential amplitude across the three epimysial electrodes. With the applied normalization procedure, the amplitude at the reference epimysial electrode corresponds to 100% and it was therefore not represented in the figure. When the reference epimysial electrode was that in the middle, the electrodes in the lateral and medial positions were both at $0.2c$ (c = muscle circumference; see above) distance from the reference. On the other end, if the reference epimysial electrode was either the lateral or the medial one, we could evaluate the amplitude at the distances of $0.2c$ and $0.4c$ along the muscle circumference. Figure 5 represents the variation in amplitude in case of single differential montage (two leftmost boxplots) or monopolar signals (two rightmost boxplots). According to the Lilliefors' test, only amplitude data from the monopolar derivation at $0.2c$ were normally distributed. For both single differential and monopolar montages, the amplitude decreased with the distance from the reference epimysial electrode ($P \ll 0.001$), with a greater decrease with distance for the single differential than the monopolar configuration. In fact, at the same distance from the reference electrode ($0.2c$ or $0.4c$) the relative amplitude was greater for the monopolar than the single differential montage ($P \ll 0.001$).

3.3. Signal quality

The average root mean square of the noise across the five channels and the eight animals was 43.5 ± 29.3 μV and 30.5 ± 19.4 μV before the first and after the last crush, respectively, for single differential montage. The corresponding values for monopolar detection were 34.8 ± 13.2 μV and 23.5 ± 11.0 μV. The corresponding average signal-to-noise

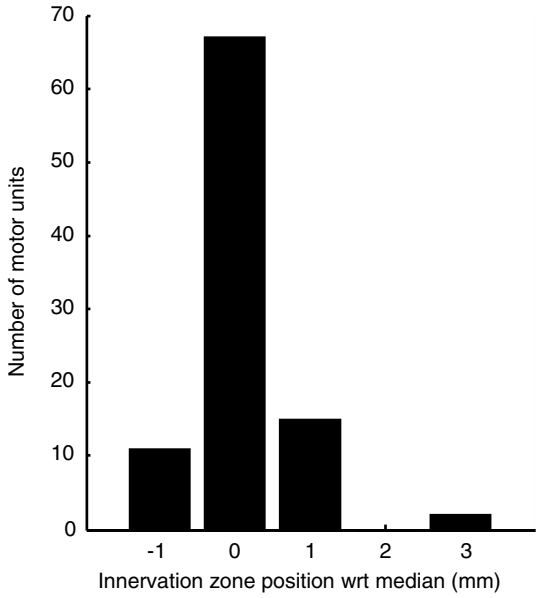

Figure 4. Spread of the innervation zone in the reinnervated muscle in Sprague-Dawley rats. The median value of the position of the innervation zone of all motor units identified in a muscle corresponds to the origin of the *x*-axis of the histogram (1 unit corresponds to the electrode inter-site distance, i.e. 1 mm). Negative and positive values correspond to distal and proximal positions with respect to the origin, respectively. The neuromuscular junctions were mainly centred about the position where the nerve was neurotized, within a 5 mm range. Images from Thy1-GFP transgenic rats (figure 3(B)) confirmed the finding about the spread of the innervation zones.

ratio across motor unit action potentials was 31.7 ± 10.2 dB and 32.4 ± 9.3 dB in the single differential and monopolar case, respectively.

4. Discussion

We investigated the use of epimysial electrodes for motor unit action potential detection in TMR muscles. We could observe the propagation of each action potential from the innervation zone to the tendon and the velocity at which the potential moved along the muscle fibers. Moreover, we reported the spread of the innervation zone along the muscle longitudinal direction and validated these data by direct imaging. These results indicate that thin-film epimysial electrodes are suitable for single motor unit recording.

4.1. Epimysial detection from TMR muscles

TMR has been introduced to increase the number of control signals in upper extremity amputees. The resulting signals are usually used for direct control of a prosthetic device. Non-invasive multi-channel electrodes have been used to record from TMR muscles (Huang *et al* 2008). In this previous study, global features were extracted from the EMG signals for prosthetic control. A recent study proposed the use of motor unit discharge timings as features for improving prosthetic control in TMR amputees (Farina *et al* 2017b). In that study, motor units were detected by advanced processing of signals recorded with multi-channel grids of surface electrodes. The deconvolution of EMG signals into the motor unit discharge timings relies on blind source separation techniques that require the availability of a relatively large number of observations (detection sites), superior to the number of sources (active motor units). However, EMG signals collected by surface electrodes vary substantially with electrode replacement, as a consequence of donning and doffing of the prosthesis and are influenced by skin conditions. These problems may be solved by invasive solutions, which additionally provide superior signal quality (Ortiz-Catalan *et al* 2014). Chronically implanting a large number of electrodes into muscles, as required for EMG automatic decomposition (Holobar and Zazula 2007, Negro *et al* 2016), may be impractical because of tissue damage. On the other hand, invasive epimysial electrodes are not inserted into muscles and at the same time bypass the subcutaneous tissues, thus increasing selectivity with respect to surface recordings. Epimysial systems may therefore be a good compromise for clinical applications. However, it has so far not been shown whether epimysial recordings have sufficient selectivity to discriminate individual motor unit discharge timings, as needed for a neural control of prosthesis. Therefore, in this study we investigated the possibility of recording motor unit activity with epimysial electrodes. The study was based on an animal preparation as first necessary preliminary step before human experiments. The results showed for the first time that epimysial recordings made with our recently developed thin-film electrodes are suitable for motor unit detection. Motor unit action potentials could be clearly distinguished from their distinct morphology (amplitude and waveform shape) and propagation velocity (figure 3(A)).

4.2. Detection volume

We analysed amplitude changes across the three epimysial electrodes. Amplitude of motor unit action potentials decreases with the distance from the source (Roeleveld *et al* 1997). Accordingly, in our study we identified the epimysial electrodes closest to each identified motor unit as those providing the action potentials with the highest amplitude. We then investigated the changes in signal amplitude with distance and with the recording montage (single differential versus monopolar) (figure 5). Amplitude decreased with the distance for both montages, but the decrease was more pronounced for single differential recordings, which therefore were more selective than monopolar ones. This result is in agreement with previous observations made with thin-film electrodes inserted intramuscularly in physiologically innervated muscles (Farina *et al* 2008). Similarly, the shape and duration of the action potentials detected in this study are qualitatively similar to those previously recorded intramuscularly from muscles with physiological innervation (Farina *et al* 2008).

In 75% of the action potentials, the single differential amplitude was below 13% of the maximal amplitude when moving by 0.4*c* from the reference electrode. This amplitude threshold approximately corresponded to the noise level. For monopolar action potentials instead, the amplitude did not

decrease to the noise level even for detection sites 0.4*c* apart, i.e. almost diametrically opposed to the source location. Thus, in this study, the recording volume corresponded to the entire muscle, given its small size (approximately 30 mm^2 cross-sectional area).

4.3. Translation to human TMR muscles

Common target muscles in the TMR procedures are the pectoralis, serratus, latissimus dorsi in case of shoulder disarticulation and biceps brachii, triceps and brachialis in case of transhumeral amputation (Miller *et al* 2008). In humans, some of these muscles (e.g. the biceps), if taken as a whole, may have a large cross-section compared to the recording volume of the electrodes used in this study. However, this detection volume would be sufficient to record from small fascicular territories corresponding to individual nerve fascicles innervating the same target muscle in advanced TMR procedures that aim at increasing the information transfer (e.g. as proposed by Bergmeister *et al* (2017)) or to record from small muscle units neurotized by peripheral nerves as in regenerative peripheral nerve interfaces (Kung *et al* 2014).

In the current experiment, the animal extremity was fixed and the relative movement between detection sites and muscle was therefore minimal. In prosthetics applications in humans, the relative movement may be greater. However, for target reinnervated muscles such as the pectoralis or the biceps, it has been shown in human experiments that it is possible to extract motor unit activity from multi-channel surface EMG signals recorded during dynamic contractions (Farina *et al* 2017b). In any case, the change in motor unit action potential shapes that may occur due to relative movement between motor units and electrodes may be compensated with appropriated decomposition algorithms (Glaser *et al* 2013).

4.4. Size of the detected population

In case of control relying on motor unit discharge timing, the number of identified motor units determines the quality of the control. Ninety-five motor units were identified in this study from eight animals, i.e. approximately 12 per animal. Imaging studies (Bergmeister *et al* 2018) showed that the lateral head of the biceps of the rat comprises approximately 30 motor units. This number may increase due to the hyperinnervation phenomenon induced by TMR (Kuiken *et al* 1995). The number of motor units we detected was about 40% or more of the motor units constituting the muscle. The fact that motor unit activity could be detected from almost diametrically opposed electrodes with respect to the fiber location suggests that all units that became active due to the nerve crushes were likely detected, including those in the deep portion of the muscle. Muscle electrical activity was elicited via progressive mechanical stimulation of the nerve. This approach does not guarantee that all motor units become active and likely the number of detected units would have been superior if more units could be activated. The measures we performed immediately after the electrode placement can be done only under general anaesthesia. In this condition, muscle activity can be elicited also via electrical stimulation but with this approach motor units are activated synchronously, making it impossible to distinguish the contribution of different motor units to the resulting compound signal. In a previous study in a rabbit preparation (Farina *et al* 2008), activity was elicited with a similar protocol as that adopted in our study. An alternative way to induce asynchronous motor unit activation is by eliciting a withdrawal reflex, for example by painful stimulation at the paw. This approach however could not be followed in our experiments due to the anaesthesia depth.

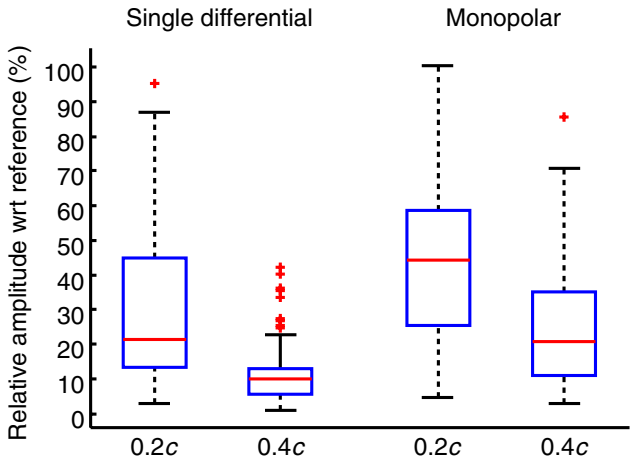

Figure 5. EMG recording selectivity. The four box plots represent the distribution of the motor unit action potential relative amplitude with respect to the reference epimysial electrode in case of single differential and monopolar detection. The electrode where the multi-channel potential had the highest amplitude was assumed to be the closest to the position of the detected motor unit and considered as reference. *c* indicates the muscle circumference. The amplitude decreased with the distance from the reference electrode, and this decrease was more pronounced in case of single differential than monopolar recordings. The outliers likely occurred when a motor unit was at comparable distances from two electrodes.

4.5. Innervation zone and conduction velocity

Exploiting single differential recordings along the muscle fibers, we were able to identify the motor unit innervation zone. We observed that the innervation zones were mainly located close to the region where the nerve was neurotized. This was confirmed by inspection of the 3D stacks of the reinnervated muscle of the Thy1-GFP rats that represent a realistic model of the reinnervation process in Sprague Dawley rats (Kemp *et al* 2013).

The average conduction velocity of the muscle fibers for the motor units of the reinnervated biceps muscle was 2.5 m s^{-1}. A previous study in Wistar rats (Kupa *et al* 1995) found average values for conduction velocity of 1.7, 1.9, and 3.0 m s^{-1} for the soleus, diaphragm, and (hindlimb) extensor digitorum longus muscles, respectively. Our results are more similar to those previously obtained for the distal extremity muscle. The fact that we could detect propagating potentials at velocity comparable with those observed in previous studies corroborates the finding that the extracted action

potentials originated from individual motor units. In Kupa *et al* (1995), the apparatus used for conduction velocity estimation included three parallel bars spaced 2.3 mm apart, from which two differential signals could be calculated. Compared to that apparatus, our epimysial electrode allows sampling the action potential along the entire muscle length, so the anatomical (innervation zone) and physiological (conduction velocity) characteristics of the muscle unit could be extracted concurrently.

5. Conclusions

We showed for the first time that multi-channel epimysial recordings are suitable for detecting single motor unit action potentials from muscles that underwent TMR surgery. Action potentials were characterized in terms of their velocity of propagation along the muscle fibers and their amplitude distribution on the muscle surface. Results showed that the electrodes' pick-up volume included the entire muscle in the rat hindlimb. These results indicate the feasibility of using epimysial electrodes for detecting motor unit activity in muscles with specific fascicular territories associated to different functions following the TMR procedure. The human translation of these findings would provide an implanted neural interface with the spinal cord.

Funding

This study was financed by the H2020-ICT Project EXTEND (No. 779982), the ERC Advanced Grant DEMOVE (No. 267888), the ERC PoC INTERSPINE (737570) and the Christian Doppler Research Association, Austrian Council for Research and Technology Development, Austrian Federal Ministry of Science, Research and Economy. None of the funding agencies were involved in the collection, analyses, and interpretation of data or writing and publication of this article.

Competing interests

The authors declare that the research was conducted in the absence of any commercial or financial relationships that could be construed as a potential conflict of interest.

ORCID iDs

Silvia Muceli https://orcid.org/0000-0002-0310-1021
Ivan Vukajlija https://orcid.org/0000-0002-7394-9474
Dario Farina https://orcid.org/0000-0002-7883-2697

References

Bergmeister K D *et al* Peripheral nerve transfers change target muscle structure and function (unpublished)
Bergmeister K D, Aman M, Riedl O, Manzano-Szalai K, Sporer M E, Salminger S and Aszmann O C 2016 Experimental nerve transfer model in the rat forelimb *Eur. Surg.* **48** 334–41
Bergmeister K D *et al* 2017 Broadband prosthetic interfaces: combining nerve transfers and implantable multichannel EMG technology to decode spinal motor neuron activity *Frontiers Neurosci.* **11** 421
Dimitrov G and Dimitrova N 1974 Extracellular potential field of a single striated muscle fibre immersed in anisotropic volume conductor *Electromyogr. Clin. Neurophysiol.* **14** 423–36
Farina D, Castronovo A M, Vujaklija I, Sturma A, Salminger S, Hofer C and Aszmann O C 2017a Common synaptic input to motor neurons and neural drive to targeted reinnervated muscles *J. Neurosci.* **37** 11285–92
Farina D and Holobar A 2016 Characterization of human motor units from surface EMG decomposition *Proc. IEEE* **104** 353–73
Farina D, Merletti R, Indino B and Graven-Nielsen T 2004 Surface EMG crosstalk evaluated from experimental recordings and simulated signals. Reflections on crosstalk interpretation, quantification and reduction *Methods Inf. Med.* **43** 30–5
Farina D, Muhammad W, Fortunato E, Meste O, Merletti R and Rix H 2001 Estimation of single motor unit conduction velocity from surface electromyogram signals detected with linear electrode arrays *Med. Biol. Eng. Comput.* **39** 225–36
Farina D, Vujaklija I, Sartori M, Kapelner T, Negro F, Jiang N, Bergmeister K, Andalib A, Principe J and Aszmann O 2017b Man/machine interface based on the discharge timings of spinal motor neurons after targeted muscle reinnervation *Nat. Biomed. Eng.* **1** 0025
Farina D, Yoshida K, Stieglitz T and Koch K P 2008 Multichannel thin-film electrode for intramuscular electromyographic recordings *J. Appl. Physiol.* **104** 821–7
Glaser V, Holobar A and Zazula D 2013 Real-time motor unit identification from high-density surface EMG *IEEE Trans. Neural Syst. Rehabil. Eng.* **21** 949–58
Hoffer J and Loeb G 1980 Implantable electrical and mechanical interfaces with nerve and muscle *Ann. Biomed. Eng.* **8** 351–60
Holobar A and Zazula D 2007 Multichannel blind source separation using convolution kernel compensation *IEEE Trans. Signal Process.* **55** 4487–96
Huang H, Zhou P, Member S, Li G and Kuiken T A 2008 An analysis of EMG electrode configuration for targeted muscle reinnervation based *IEEE Trans. Neural Syst. Rehabil. Eng.* **16** 37–45
Kapelner T, Negro F, Aszmann O C and Farina D 2018 Decoding motor unit activity from forearm muscles: perspectives for myoelectric control *IEEE Trans. Neural Syst. Rehabil. Eng.* **26** 244–51
Kemp S W P, Phua P D, Stanoulis K N, Wood M D, Liu E H, Gordon T and Borschel G H 2013 Functional recovery following peripheral nerve injury in the transgenic Thy1-GFP rat *J. Peripher. Nervous Syst.* **18** 220–31
Kuiken T A, Childress D S and Rymer W Z 1995 The hyper-reinnervation of rat skeletal muscle *Brain Res.* **676** 113–23
Kuiken T A, Lock B A, Lipschutz R D, Miller L A, Stubblefield K A and Englehart K B 2009 Targeted muscle reinnervation for real-time myoelectric control of multifunction artificial arms *J. Am. Med. Assoc.* **301** 619–28
Kuiken T A, Miller L A, Lipschutz R D, Lock B A, Stubblefield K, Marasco P D, Zhou P and Dumanian G A 2007 Targeted reinnervation for enhanced prosthetic arm function in a woman with a proximal amputation: a case study *Lancet* **369** 371–80
Kung T A, Langhals N B, Martin D C, Johnson P J, Cederna P S and Urbanchek M G 2014 Regenerative peripheral nerve interface viability and signal transduction with an implanted electrode *Plast. Reconstructive Surg.* **133** 1380–94
Kupa E J, Roy S H, Kandarian S C and De Luca C J 1995 Effects of muscle fiber type and size on EMG median frequency and conduction velocity *J. Appl. Physiol.* **79** 23–32

Luu B L, Muceli S, Saboisky J P, Farina D, Héroux M E, Bilston L E, Gandevia S C and Butler J E 2018 Motor unit territories in human genioglossus estimated with multichannel intramuscular electrodes *J. Appl. Physiol.* **124** 664–71

Masuda T, Miyano H and Sadoyama T 1983 The propagation of motor unit action potential and the location of neuromuscular junction investigated by surface electrode arrays *Electroencephalogr. Clin. Neurophysiol.* **55** 594–600

McGill K C, Lateva Z C and Marateb H R 2005 EMGLAB: an interactive EMG decomposition program *J. Neurosci. Methods* **149** 121–33

Merletti R, Farina D and Gazzoni M 2003 The linear electrode array: a useful tool with many applications *J. Electromyogr. Kinesiol.* **13** 37–47

Miller L A, Stubblefield K A, Lipschutz R D, Lock B A and Kuiken T A 2008 Improved myoelectric prosthesis control using targeted reinnervation surgery: a case series *IEEE Trans. Neural Syst. Rehabil. Eng.* **16** 46–50

Moore A M *et al* 2012 A transgenic rat expressing green fluorescent protein (GFP) in peripheral nerves provides a new hindlimb model for the study of nerve injury and regeneration *J. Neurosci. Methods* **204** 19–27

Muceli S, Poppendieck W, Negro F, Yoshida K, Hoffmann K P, Butler J E, Gandevia S C and Farina D 2015 Accurate and representative decoding of the neural drive to muscles in humans with multi-channel intramuscular thin-film electrodes *J. Physiol.* **593** 3789–804

Negro F, Muceli S, Castronovo A M, Holobar A and Farina D 2016 Multi-channel intramuscular and surface EMG decomposition by convolutive blind source separation *J. Neural Eng.* **13** 026027

Ortiz-Catalan M, Hakansson B and Branemark R 2014 An osseointegrated human-machine gateway for long-term sensory feedback and motor control of artificial limbs *Sci. Transl. Med.* **6** 257re6

Roeleveld K, Stegeman D F, Vingerhoets H M and Van Oosterom A 1997 The motor unit potential distribution over the skin surface and its use in estimating the motor unit location *Acta Physiol. Scand.* **161** 465–72

Vujaklija I, Muceli S, Bergmeister K, Aszmann O C and Farina D 2017 Prospects of neurorehabilitation technologies based on robust decoding of the neural drive to muscles following targeted muscle reinnervation *Converging Clinical and Engineering Research on Neurorehabilitation II. Biosystems & Biorobotics* vol 15 ed J Ibáñez *et al* (Cham: Springer) pp 1359–63